Christian Würth*, Daniel Geißler, and Ute Resch-Genger*

Quantification of Anisotropy-Related Uncertainties in Relative Photoluminescence Quantum Yield Measurements of Nanomaterials – Semiconductor Quantum Dots and Rods

Abstract: In order to assess the anisotropy-related uncertainties of relatively determined photoluminescence quantum yields (Φ_{PL}) of molecular emitters and luminescent nanomaterials, we compared Φ_{PL} values measured without and with polarizers using magic angle conditions and studied systematically the dependence of the detected emission intensity on the polarizer settings for samples of varying anisotropy. This includes a dispersion of a spherical quantum dot (QD) with an ideally isotropic emission, a solution of a common small organic dye in a fluid solvent as well as dispersions of elongated quantum dot rods (QDR) with an anisotropic luminescence and a small organic dye in a rigid polymeric matrix, as ideally anisotropic emitter. Our results show that for instruments lacking polarizers, anisotropy-related measurement uncertainties of relative photoluminescence quantum yields can amount to more than 40%, with the size of these systematic errors depending on the difference in emission anisotropy between the sample and the standard.

Keywords: Photoluminescence, Quantum Yield, Emission Anisotropy, Quantum Dot Rod, Quantum Dot, Dye.

DOI 10.1515/zpch-2014-0626
Received September 24, 2014; accepted October 6, 2014

Dedicated to Horst Weller on the occasion of his 60th birthday

***Corresponding author: Christian Würth, Ute Resch-Genger,** BAM – Federal Institute for Materials Research and Testing, Division 1.10 Biophotonics, Richard-Willstätter-Str. 11, 12489 Berlin, Germany, e-mail: christian.wuerth@bam.de, ute.resch@bam.de
Daniel Geißler: BAM – Federal Institute for Materials Research and Testing, Division 1.10 Biophotonics, Richard-Willstätter-Str. 11, 12489 Berlin, Germany

1 Introduction

In the last decades, photoluminescence (PL) techniques developed into some of the most popular analytical tools in the life and material sciences [1–8] due to their comparative simplicity, the multitude of parameters provided, and the extraordinary sensitivity down to the single molecule level. This led to the development of an ever growing toolbox of fluorescent reporters to choose from, ranging from small organic dyes and metal-ligand complexes over fluorescent proteins and semiconductor nanocrystals to all types of fluorophore-labeled nanoparticles and up-conversion nanophosphors. Despite the popularity of PL techniques, it is often neglected that all PL measurements are affected by instrument- and sample-related polarization effects. This can distort the intensity and spectral shape of the resulting emission spectra. [9, 10]

PL measuring systems contain several potential sources of polarized light: a) excitation sources like lasers and light emitting diodes (LEDs) always provide polarized light, and b) some optical components (especially monochromator gratings) reveal polarization-dependent transmission and reflection efficiencies making the excitation partially polarized even with otherwise isotropic light sources. Also, c) detectors can show weak polarization effects typically in the range of a few percent. [11] For emission spectrometers and microscopes equipped with conventional light sources such as xenon lamps providing an isotropic emission, the size of instrument-related polarization effects is largely determined by the type of monochromator and gratings employed. Hence, the excitation light in PL measuring systems is commonly at least partly polarized, with the degree of polarization depending on the instrument.

As polarization effects can affect all types of intensity-related PL information, they must be considered for the determination of the photoluminescence quantum yield (Φ_{PL}). Φ_{PL} is a measure for the efficiency of the conversion of absorbed into emitted photons and thus, a spectroscopic key parameter for fluorophore performance evaluation and comparison. Many photophysical studies rely on Φ_{PL} measurements, e.g., for the determination of radiative rate constants, and knowledge of Φ_{PL} is crucial for the calculation of Förster resonance energy transfer (FRET) efficiencies. For nanocrystalline materials like semiconductor quantum dots and rods, the size of Φ_{PL} presents also a criterion for particle quality, i.e., the passivation of surface defects. [10, 12, 13] Although for accurate Φ_{PL} measurements, the use of polarizers set to magic angle conditions (excitation polarizer set to 0°, emission polarizer set to 54.7°) has been recommended, [9, 14] the emission spectra and Φ_{PL} values of many emitters are still often measured without

polarizers, even for systems that could reveal a partly or even strongly polarized emission.

A measure for sample- or material-related polarization effects provides the emission anisotropy r, see Equation (1), which is a property of a fluorophore in a defined environment. [2, 15] r reveals the average angular displacement of the fluorophore between absorption and subsequent emission of a photon and depends on the extent to which excited fluorophores rotate during their excited-state lifetime. Due to photoselection, only fluorophores with transition dipole moments parallel to the polarization direction of the incident light can absorb light and are accordingly excited. The emission anisotropy is also a common tool to assess the rotational freedom of dyes, and thus, e.g., dye-biomolecule interactions, and to study energy transfer. [2] However, care must be taken as r depends also strongly on the photoluminescence decay time τ. [16, 17] Hence for the interpretation of emission anisotropy studies, the measurement of τ is generally beneficial. Anisotropic emission can be expected for most fluorophores with very short PL decay times (shorter than a few 100 ps), for all organic dyes placed in a rigid confined environment (e.g., in highly viscous solvents, embedded in a solid matrix such as polymers or zeolites, or bound to large macro- or biomolecules), as well as for large fluorophores like most organic NIR dyes (even in fluid solvents). [2, 18, 19] Moreover, rod-shaped nanomaterials like elongated semiconductor nanocrystals (quantum rods, QRs) typically display an anisotropic emission. [20–23]

The increasing importance in measuring Φ_{PL} of anisotropic emitters like dye-biomolecule conjugates and luminescent nanomaterials with e.g., a shape-induced anisotropy encouraged us to study polarization-induced changes of the detection efficiency of a commercial fluorometer and to quantify polarization-related uncertainties of Φ_{PL} measurements. For this purpose, we chose quantum dot-rods (QDRs), a novel class of semiconductor nanocrystals increasingly used as reporters for bioanalytical applications and medical diagnostics [28–30] and active materials for plasma displays, which consist of a spherical core and an elongated shell. QDRs possess unique photophysical properties, such as size-tunable absorption and emission spectra (dependent on the core diameter), huge absorption cross-sections, and narrow, symmetric emission bands like spherical quantum dots (QDs). [24–27] In addition, QDRs can have even higher extinction coefficients and brightness compared to QDs. Moreover, most importantly for our study, the emission anisotropy of QDRs depends on their aspect ratios. [20–23]

In order to assess anisotropy-related uncertainties, we compared Φ_{PL} measured without and with polarizers using magic angle conditions and studied systematically the dependence of the detected emission intensities on the polarizer settings used for samples with different anisotropies and the effect on relatively determined Φ_{PL}. This included a dispersion of spherical QDs with ideally isotropic

emission, the solution of a small organic dye in a fluid non-interacting solvent (Rh101 in ethanol) with nearly isotropic emission, a dispersion of elongated QDRs with significant anisotropic emission due to the elongated shape of the QDRs, and a small organic dye embedded in a solid polymer matrix showing nearly the highest possible emission anisotropy. [31]

2 Experimental and material section

2.1 Materials

The QD and QDR were synthesized by Dipl.-Chem. Christopher Wolter from the group of professor Horst Weller (University of Hamburg, Institute of Physical Chemistry) according to a procedure described previously. [20] The QDR was a CdSe/CdS core/shell quantum dot-rod made from a spherical CdSe core (diameter 4 nm). Its rod-shaped CdS shell had a length of 53.4 nm and an aspect ratio of 12. The QD had a diameter of 14 nm and was made from the same CdSe core as the QDR with a CdS shell thickness of 5 nm. Rhodamine B incorporated in polymethylmethycrylate (PMMA) was purchased from Starna as cuvette shaped polymer block of 10 × 10 × 45 mm with polished facets. Rhodamine 101 (Rh101, batch number 019502) was purchased from Lambda Physics.

Solvents: All QD and QDR samples were provided as stock solutions in hexane and were diluted with hexane for the spectroscopic studies. Rh101 was dissolved in ethanol. Both solvents were of spectroscopic grade and purchased from Sigma Aldrich.

2.2 Instrumentation

Emission measurements: Steady-state emission anisotropies were recorded on a FLS920 fluorescence spectrometer (Edinburgh Instruments), equipped with Glan-Thompson prism polarizers and a subtractive Czerny-Turner double grating emission monochromator.

Absorption measurements: Absorption spectra were obtained on a Cary 5000 UV-Vis-NIR spectrometer (Varian Inc., Agilent Technologies) with a spectral bandwidth and step size of 1 nm. The accuracy of the intensity and wavelength scale of this instrument is regularly controlled with certified absorption standards from Hellma GmbH.

2.3 Methods

The emission anisotropy r of a sample is caused by dipole moments of an ensemble of fluorophores that are not randomly orientated or by a small rotational diffusion time of the emitter compared to its excited state lifetime. r is commonly calculated from the sample's spectrally uncorrected PL intensities $I_{0°/0°}$ and $I_{0°/90°}$ using vertically (0°) polarized excitation, and emission polarizers set to 0° and 90°, respectively (see Equation 1). [14]

$$r = \frac{I_{0°/0°}(\lambda_{em}) - G^{0°,90°}(\lambda_{em})I_{0°/90°}(\lambda_{em})}{I_{0°/0°}(\lambda_{em}) + 2G^{0°,90°}(\lambda_{em})I_{0°/90°}(\lambda_{em})} \quad (1)$$

The G^{α_1,α_2} factor in a 0°/90° measurement geometry is a wavelength-dependent correction factor to account for the different transmission efficiencies for polarized light of the optical components and the detector in the emission channel. It represents the difference of the relative spectral responsivity between two different positions of the polarizer in the detection channel. To determine the G^{α_1,α_2} factor, the excitation polarizer has to be set to 90° (horizontally polarized excitation) to ensure that only unpolarized light emitted by the sample is detected.

$$G^{\alpha_1,\alpha_2}(\lambda_{em}) = \frac{I_{90°/\alpha_1}(\lambda_{em})}{I_{90°/\alpha_2}(\lambda_{em})} \quad (2)$$

The correction factor $G^{0°,90°}$ (superscripts indicate the two positions of the emission polarizer α_1 and α_2) for the calculation of r can be determined from the sample´s emission intensities $I_{90°/0°}$ and $I_{90°/90°}$ using horizontally polarized excitation, and emission polarizers set to 0° and 90°, respectively (see Equation 2). [14] Alternatively to uncorrected emission spectra and G factors, spectrally corrected emission spectra can be used. [14].

Relative Φ_{PL} measurements: The PL quantum yield can be measured with optical methods relatively to a quantum yield standard of known Φ_{PL}, typically using identical excitation wavelengths for sample and standard and closely matching absorbances at the excitation wavelength. For relative measurements, instrument- and fluorophore-related polarization effects can be controlled with polarizers in the excitation and emission channel. If not otherwise stated, we recorded steady state PL spectra with so-called magic angle conditions (excitation polarizer set to 0° and emission polarizer set to 54.7°) to render detected emission intensities independent of the sample's emission anisotropy. [32] All emission spectra were corrected for emission from the solvent and dark counts from the detector (blank correction) and for instrument-specific contributions (emission correction), as described elsewhere. [33] The Φ_{PL} values of all samples were

calculated relatively to rhodamine 101 (Rh101, $\Phi_{PL} = 0.915$ [9]) employing the formula of Demas and Crosby, see Equation (3) [34]:

$$\Phi_{PL,x} = \Phi_{PL,st} \frac{F_x(\lambda_{em,x})}{F_{st}(\lambda_{em,st})} \frac{f_{st}(\lambda_{ex,st})}{f_x(\lambda_{ex,x})} \frac{n_x^2}{n_{st}^2} \tag{3}$$

Herein, the subscripts x and st denote sample and standard, ex and em denote excitation and emission wavelength(s), $\Phi_{PL,st}$ equals the PL quantum yield of the standard, $f(\lambda_{ex})$ presents the absorption factor at the excitation wavelength, and n is the refractive index of the respective solvent. F presents the integrated spectral fluorescence photon flux at the detector that is obtained from the blank corrected signal of the emission detector $I_{0°/55°}(\lambda_{em})$ divided by the photon energy hc_0/λ_{em} and by the relative spectral responsivity $s^{55°}(\lambda_{em})$ determined with the emission polarizer to 54.7°. This quotient was integrated over the emission wavelength ranges displayed in the left panel of Figure 1 (see Equation 4).

$$F = (hc_0)^{-1} \int_{\lambda_{em_1}}^{\lambda_{em_2}} \frac{I_{0/55°}(\lambda_{em})}{s^{55°}(\lambda_{em})} \lambda_{em} d\lambda_{em} \tag{4}$$

For all samples (QD and QRD in hexane, RhB in PMMA and Rh101 in EtOH), the same excitation wavelength of $\lambda_{ex} = 530$ nm was used. Hence, the photon fluxes at the sample position for standard and sample at the chosen excitation wavelengths are identical. The refractive indices used were $n_x = 1.375$ (for QD and QDR in hexane), $n_x = 1.491$ for the polymer block (RhB in PMMA) and $n_{st} = 1.364$ (for Rh101 in ethanol).

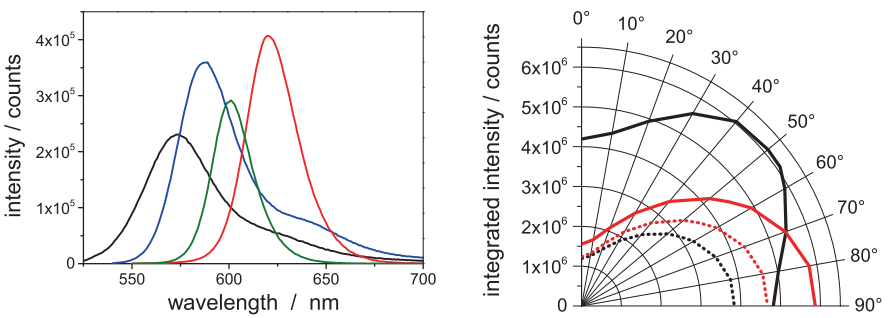

Figure 1: Left: Spectrally corrected emission spectra (I_c^{55}, $\lambda_{ex} = 530$ nm) of the QDR (green) and the QD (red) dispersed in hexane, RhB incorporated in PMMA (black), and Rh101 dissolved in ethanol (blue). Right: Integrated emission intensities obtained from the uncorrected emission spectra with the excitation polarizer set to 0° ($I_{0°/0°...90°}$, solid lines) and 90° ($I_{90°/0°...90°}$, dotted lines), respectively, in dependence of the angle of the emission polarizer for the QD in hexane (red) and RhB in PMMA (black).

For fluorescence spectrometers equipped with polarizers, the relative spectral responsivity $s(\lambda_{em})$ is often determined for magic angle conditions. If emission spectra are recorded with emission polarizer settings differing from the settings used to determine $s(\lambda_{em})$, polarization effects in the detection channel have to be considered. Hence, we use the G^{α_1,α_2} factor to determine the difference of the relative spectral responsivity between the actual position of the emission polarizer (α_2) and the magic angle conditions ($\alpha_1 = 54.7^\circ$) and to calculate the corrected emission spectra $I_c^{\alpha_2}$. The integrated spectral fluorescence photon flux determined with an angle (α_2) of the emission polarizer can be calculated by Equation (5).

$$\begin{aligned} F^{\alpha_2} &= (hc_0)^{-1} \int_{\lambda_{em_1}}^{\lambda_{em_2}} I_c^{\alpha_2}(\lambda_{em})\lambda_{em} d\lambda_{em} \\ &= (hc_0)^{-1} \int_{\lambda_{em_1}}^{\lambda_{em_2}} \frac{I_{0^\circ/\alpha_2}(\lambda_{em})}{s^{55^\circ}(\lambda_{em})} G^{55^\circ,\alpha_2}(\lambda_{em})\lambda_{em} d\lambda_{em} \end{aligned} \quad (5)$$

Equation (4) is a special case of Equation (5) with $G^{55^\circ,\alpha 2}$ equaling 1.

3 Results and discussion

Recommended settings for the determination of Φ_{PL} of all types of fluorescent reporters are the magic angle conditions, where the excitation polarizer is set to 0° and the emission polarizer to 54.7°, as this renders detected emission intensities independent of the emission anisotropy of the sample. The spectrally corrected emission spectra of the different emittters recorded under this condition are displayed in Figure 1 (left panel). Since all fluorophores emit in a wavelength region between 530 and 700 nm, the same G^{α_1,α_2} factors can be used for all samples.

To determine Φ_{PL} or the emission anisotropy, either the spectral responsivity $s(\lambda_{em})$ or the G^{α_1,α_2} factors have to be considered for the polarization dependence of the spectral responsivity of the emission channel for the polarizer settings used. To demonstrate the considerable influence of polarization effects on measured emission intensities, the integrated emission intensities with the excitation polarizer set to 90° (necessary to calculate the G^{α_1,α_2} factors) are plotted in Figure 1 (right panel, dotted lines) for RhB and the QD sample in dependence of the angle of the emission polarizer. As follows from this figure, the detection channel of our fluorometer shows the highest sensitivity at an angle of 90°. The factors between the integral emission intensities at 0° and 90° are 3.2 and 3.8 for RhB and the QD,

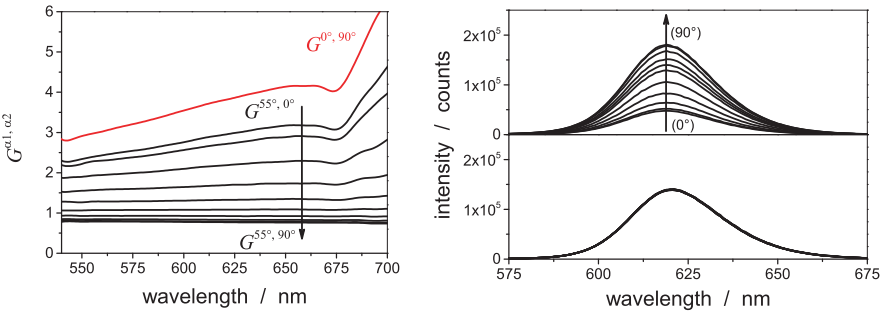

Figure 2: Left: Wavelength dependence of the correction factors G^{α_1,α_2} (see Equation 2) for $\alpha_1 = 0^\circ$, $\alpha_2 = 90^\circ$ (red) and $\alpha_1 = 55^\circ$, $\alpha_2 = 0...90^\circ$ (black) combinations of the emission polarizer (excitation polarizer set to 90°). Right: Uncorrected ($I_{0^\circ/0^\circ...90^\circ}$, top) and corrected ($I_c^{0^\circ...90^\circ}$, bottom) emission spectra (see Equation 5) of the QD determined with the emission polarizer set to $0^\circ \ldots 90^\circ$ (excitation polarizer set to 0°).

respectively, indicating already the wavelength dependence of the G^{α_1,α_2} factor. In Figure 1 (right panel), also the integral emission intensities in dependence of the angle of the emission polarizer are shown for a 0° excitation polarizer position. For the dye in a rigid matrix, the highest emission intensities were detected at 50° indicating a high emission anisotropy, as expected for a fluorophore with strongly reduced rotational and translational mobility. In contrast to the QD in hexane, which gave the highest emission intensity at 90° with a trend direct proportional to the 90° excitation, indicating an ideal isotropic emission.

As follows from Equation (5), the anisotropy of both sample and standard affect the relatively measured Φ_{PL} due to the influence of polarization effects on the measured emission intensities. To demonstrate the extent of these effects for different samples of low and high emission anisotropy, we determined the wavelength-dependent $G^{0^\circ,90^\circ}$ factor from the emission spectra $I_{90^\circ/0^\circ}$ and $I_{90^\circ/90^\circ}$ (see Figure 2, red line). In addition, we obtained the emission anisotropies of all samples from the emission spectra $I_{0^\circ/0^\circ}$ and $I_{0^\circ/90^\circ}$ as well as the respective Φ_{PL} values from the emission spectra $I_{0^\circ/55^\circ}$ and from the emission spectra recorded without polarizers in the excitation and emission channel, respectively.

Table 1 summarizes the resulting emission anisotropies and the relatively measured Φ_{PL} using Rh101 in ethanol as reference ($\Phi_{PL} = 0.915$). The emission of the QD in hexane ($r = 0$) and Rh101 in ethanol ($r = 0.02$) are more or less isotropic, whereas RhB in PMMA shows an almost ideal emission anisotropy of $r = 0.37$. The QDR reveals a comparably high anisotropy of $r = 0.18$ that is shaped-induced. The anisotropies correlate directly with the deviations between the Φ_{PL} values determined with magic angle conditions and without polarizers (see Table 1). For

Table 1: Emission anisotropies, Φ_{PL} determined with and without polarizers and their relative deviation. The bold values indicate the standard used for the relative Φ_{PL} measurements.

Dye (solvent/matrix)	r	Φ_{PL} (no polarizers)	Φ_{PL} (0°/54.7°)	Rel. dev [%]
QD (hexane)	0	0.785	0.767	−2.2
Rh101 (ethanol)	**0.02**	**0.915**	**0.915**	**0.0**
QDR (hexane)	0.18	0.509	0.599	17.6
RhB (PMMA)	0.37	0.525	0.758	44.3

PL measurements without polarizers, already the small emission anisotropy of Rh101 in ethanol causes a deviation of approx. −2% for the relatively measured Φ_{PL} of the ideal isotropically emitting QD. This deviation increases with increasing anisotropy of the samples to ca. 18% for the QDR and to more than 44% for the solid anisotropically emitting sample.

Only magic angle conditions (0°/54.7°) allow for the determination of emission intensities independent of the orientation and excited state lifetimes of the samples' transition dipoles moments. If different polarizer settings are employed, the emission intensities or photon fluxes used for the calculation of Φ_{PL} are not proportional to the average excitable dipoles in the sample, although the spectral responsivity of the detection channel is considered. To demonstrate this and the resulting under- or overestimation of Φ_{PL}, we determined the respective G^{55°,α_2} factors to correct for the polarization-induced changes of the spectral responsivity of the detection channel compared to an angle of 54.7° of the emission polarizer (see Equation (5) and Figure 2, left panel, black lines). The G^{55°,α_2} factors are strongly wavelength and angle dependent as shown in Figure 2 (left panel). The wavelength dependence of $G^{55^\circ,90^\circ}$ is rather flat in the wavelength range of 540 nm to 700 nm and has a negative slope, in contrast to that of $G^{55^\circ,0^\circ}$ revealing a positive slope and strong features around 675 nm. To demonstrate the influence of the G^{55°,α_2} factors on the measured emission intensities and the spectral shape of the emission spectra, we compared the uncorrected emission spectra $I_{0^\circ/0^\circ\ldots90^\circ}$ of the isotropically emitting QD (Figure 2 right panel, top) with the respective G^{55°,α_2} factor-corrected emission spectra (Figure 2, right panel, bottom) that consider polarization-induced changes of the spectral responsivity of the detec-

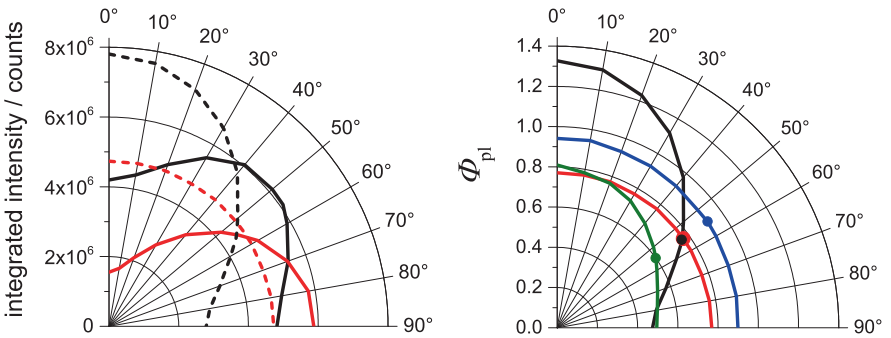

Figure 3: Left: Integrated intensities of uncorrected (I_c^{55}, solid lines) and corrected ($I_c^{0^\circ\ldots90^\circ}$, dotted lines) emission spectra (see Equation 5) of the QD in hexane (red) and RhB in PMMA (black), measured with the excitation polarizer set to 0° in dependence of the angle of the emission polarizer. Right: Φ_{PL} of the QDR (green) and the QD (red) in hexane, RhB incorporated in PMMA (black), and Rh101 in ethanol (blue) in dependence of the angle of the emission polarizer (0° excitation polarizer), using a nearly isotropically emitting reference, i.e., Rh101 in ethanol. Magic angle conditions ($0^\circ/54.7^\circ$) are indicated by dots (see also Table 1).

tion channel. This gives a perfect match of all emission spectra for this isotropic emitter.

The corrected and uncorrected integrated emission intensities obtained for the isotropically emitting QD and the strongly anisotropically emitting RhB sample for an excitation polarizer position of 0° are shown in Figure 3 (left panel). RhB in PMMA reveals the strongest corrected emission (highest detectable photon flux) in a 0° polarization plane, exceeding the signal in the 90° polarization plane by a factor of 2.8. The QD shows an unpolarized emission.

The Φ_{PL} calculated from the G^{55°,α_2} factor-corrected emission spectra are shown in Figure 3 (right panel) in dependence of the angle of the detection polarizer. Only for the QD, the resulting Φ_{PL} is independent of the polarizer position. Even for Rh101 in ethanol showing a very small anisotropy ($r = 0.02$), the detected photon flux changes slightly and Φ_{PL} determined relatively to the magic angle condition ($\Phi_{PL} = 0.915$) varies between 0.942 and 0.9. For the QDR in hexane ($r = 0.18$) and RhB in PMMA ($r = 0.37$), showing nearly the same PL quantum yields for the magic angle conditions, the Φ_{PL} resulting for positions of the emission polarizer between 90° and 0° vary between 0.495 and 0.809 (variation of 60%) and 0.474 and 1.32 (variation of 180%), respectively. For the samples shown here, the use of unsuited polarizer settings results in a Φ_{PL} underestimation of 21% (QDR) and 60% (RhB) for the 90° emission polarizer position and in a Φ_{PL} overestimation of 35% (QDR) and 74% (RhB) for the 0° emission polarizer position, respectively, compared to the respective Φ_{PL} obtained with magic angle con-

ditions. These considerable deviations clearly underline the importance for measurements with polarizers using magic angle conditions for reliable relative Φ_{PL} measurements. Although the exact size of these effects is instrument-dependent, similar deviations are to be expected for other fluorescence measuring systems.

4 Conclusion

In summary, we demonstrated that for relative measurements of photoluminescence quantum yields (Φ_{PL}) without polarizers, the emission anisotropies of the standard and sample can considerably affect the resulting Φ_{PL} values. This can lead to significant uncertainties of Φ_{PL} data, the size of which depends on the difference in emission anisotropy of sample and standard. Although the size of emission anisotropy- and polarization-related effects are instrument-specific, depending mainly on the type of monochromator gratings, which typically determines the polarization sensitivity of the fluorescence measuring system. For the fluorometer used here and the sample with the highest emission anisotropy, uncertainties of more than 40% were obtained for measurements without polarizers. Maximum possible uncertainties of over 70% can be reached in a worst case scenario (estimated from the $0^{\circ}/0^{\circ}$ measurement geometry). For instruments lacking polarizers, polarization-related systematic uncertainties correlate directly with the size of the anisotropy of the sample, with minimum effects only resulting for samples with negligibly small emission anisotropies. For relative Φ_{PL} measurements of samples with higher anisotropies, sample-standard pairs with closely matching anisotropies are favorable, thereby reducing the influence of polarization effects, at least for samples with randomly orientated dipole moments. For instruments equipped with polarizers, use of magic angle conditions is strongly recommended for relative measurements of Φ_{PL} standards. Simultaneously, this underlines the need to provide emission anisotropies for solutions of recommended quantum yield standards and may render the development of anisotropic Φ_{PL} standards attractive.

Acknowledgement: We gratefully acknowledge financial support from the Federal Ministry of Economics and Technology (MNPQ program, project BMWI-11/12), from the European Comission (EMRP project NEW03 NanoChOp), and from the DFG (project RE1203/12-1). We are much obliged to Professor Horst Weller, Institute of Physical Chemistry of the University of Hamburg, for the provision of the QD and QRD samples, which were synthesized by Dipl.-Chem. Christopher Wolter.

References

1. W. T. Mason, *Fluorescent and Luminescent Probes for Biological Activity*, 2nd edn., Academic Press, London, UK (1999).
2. J. R. Lakowicz, *Principles of Fluorescence Spectroscopy*, 3rd edn., Springer Science + Business Media, LLC, New York (2006).
3. R. Weissleder and M. J. Pittet, Nature **452** (2008) 580.
4. H. Kobayashi, M. Ogawa, R. Alford, P. L. Choyke, and Y. Urano, Chem. Rev. **110** (2010) 2620.
5. M. Y. Berezin and S. Achilefu, Chem. Rev. **110** (2010) 2641.
6. L. D. Lavis and R. T. Raines, ACS Chem. Biol. **3** (2008) 142.
7. Resch-U. Genger, M. Grabolle, S. Cavaliere-Jaricot, R. Nitschke, and T. Nann, Nat. Methods **5** (2008) 763.
8. K. E. Sapsford, L. Berti, and I. L. Medintz, Angew. Chem. Int. Edit. **45** (2006) 4562.
9. C. Würth, M. Grabolle, J. Pauli, M. Spieles, and U. Resch-Genger, Nat. Protoc. **8** (2013) 1535.
10. M. Grabolle, M. Spieles, V. Lesnyak, N. Gaponik, A. Eychmüller, and U. Resch-Genger, Anal. Chem. **81** (2009) 6285.
11. U. Resch-Genger, D. Pfeifer, C. Monte, W. Pilz, A. Hoffmann, M. Spieles, K. Rurack, J. Hollandt, D. Taubert, B. Schonenberger, and P. Nording, J. Fluoresc. **15** (2005) 315.
12. S. Leubner, S. Hatami, N. Esendemir, T. Lorenz, J. O. Joswig, V. Lesnyak, S. Recknagel, N. Gaponik, U. Resch-Genger, and A. Eychmüller, Dalton T. **42** (2013) 12733.
13. S. Leubner, R. Schneider, A. Dubavik, S. Hatami, N. Gaponik, U. Resch-Genger, and A. Eychmuller, J. Mater. Chem. C **2** (2014) 5011.
14. B. Valeur, in: *Molecular Fluorescence: Principles and Applications*, Wiley-VCH Verlag GmbH, Weinheim (2001) (http://www.wiley-vch.de/publish/en/books/bySubjectCH00/ISBN3-527-32837-8/?sID=adk7lgdivvki34ause91ocn403).
15. D. M. Jameson and J. A. Ross, Chem. Rev. **110** (2010) 2685.
16. B. J. Harvey, C. Perez, and M. Levitus, Photoch. Photobio. Sci. **8** (2009) 1105.
17. B. J. Harvey and M. Levitus, J. Fluoresc. **19** (2009) 443.
18. T. J. V. Prazeres, A. Fedorov, S. P. Barbosa, J. M. G. Martinho, and M. N. Berberan-Santos, J. Phys. Chem. A **112** (2008) 5034.
19. L. Linck, P. Kapusta, and U. Resch-Genger, Photoch. Photobio. **88** (2012) 867.
20. D. V. Talapin, R. Koeppe, S. Gotzinger, A. Kornowski, J. M. Lupton, A. L. Rogach, O. Benson, J. Feldmann, and H. Weller, Nano Lett. **3** (2003) 1677.
21. J. Hu, L.-S. Li, W. Yang, L. Manna, L.-W. Wang, and A. P. Alivisatos, Science **292** (2001) 2060.
22. I. Hadar, G. B. Hitin, A. Sitt, A. Faust, and U. Banin, J. Phys. Chem. Lett. **4** (2013) 502.
23. D. B. Tice, D. J. Weinberg, N. Mathew, R. P. H. Chang, and E. A. Weiss, J. Phys. Chem. C **117** (2013) 13289.
24. A. L. Efros and M. Rosen, Annu. Rev. Mater. Sci. **30** (2000) 475.
25. C. J. Murphy and J. L. Coffer, Appl. Spectrosc. **2002**, *56*, 16A.
26. L. Carbone, C. Nobile, M. De Giorgi, F. D. Sala, G. Morello, P. Pompa, M. Hytch, E. Snoeck, A. Fiore, I. R. Franchini, M. Nadasan, A. F. Silvestre, L. Chiodo, S. Kudera, R. Cingolani, R. Krahne, and L. Manna, Nano Lett. **7** (2007) 2942.
27. J. Dimitrijevic, L. Krapf, C. Wolter, C. Schmidtke, J.-P. Merkl, T. Jochum, A. Kornowski, A. Schuth, A. Gebert, G. Huttmann, T. Vossmeyer, and H. Weller, Nanoscale **6** (2014) 10413.

28. D. Gao, P. Zhang, Z. Sheng, D. Hu, P. Gong, C. Chen, Q. Wan, G. Gao, and L. Cai, Adv. Funct. Mater. **24** (2014) 3897.
29. K.-T. Yong, R. Hu, I. Roy, H. Ding, L. A. Vathy, E. J. Bergey, M. Mizuma, A. Maitra, and P. N. Prasad, ACS Appl. Mater. Interfac. **1** (2009) 710.
30. K.-T. Yong, J. Qian, I. Roy, H. H. Lee, E. J. Bergey, K. M. Tramposch, S. He, M. T. Swihart, A. Maitra, and P. N. Prasad, Nano Lett. **7** (2007) 761.
31. C. Würth, K. Hoffmann, T. Behnke, M. Ohnesorge, and U. Resch-Genger, J. Fluoresc. **21** (2011) 953.
32. K. D. Mielenz, E. D. Cehelnik, and R. L. McKenzie, J. Chem. Phys. **64** (1976) 370.
33. C. Würth, M. Grabolle, J. Pauli, M. Spieles, and U. Resch-Genger, Anal. Chem. **83** (2011) 3431.
34. G. A. Crosby and J. N. Demas, J. Phys. Chem. **75** (1971) 991.

Christian Würth and Daniel Geißler are equally contributing authors.